

NUMERICAL ANALYSIS OF THE PERFORMANCE OF CYLINDRICAL CAVITIES AT MICROWAVE FREQUENCIES

By

A. O. AKALA*, A. B. ADELOYE* and E.O. SOMOYE**

*Department of Physics, University of Lagos, Akoka, Yaba, Lagos, Nigeria

**Department of Physics, Lagos State University, Ojo, Lagos, Nigeria

ABSTRACT

This paper presents how numerical approach can be used to analyze the performance of cylindrical cavities at microwave frequencies. The thrust of the paper is to provide a useful guide for the engineering designs of high performance resonant cavity. Bessel differential equation is used to discuss the theory of cylindrical resonant cavity. The distribution of electric fields inside the cavity was numerically computed. Thereafter, numerical simulation for several excitation modes was carried out. Overall, critical analysis of the results from the numerical computations and simulations reveal that $L/R > 1.5$ is a better scale for a robust resonant cavity. This scale shows reasonable consistency with known values. Proper choice of modes (mode matching) is also a significant index for designing a robust system.

Keywords: Cylindrical cavity; Bessel differential equation; Resonant frequency; Excitation mode.

NOTATIONS

ϵ \equiv Dielectric permittivity

μ \equiv Permeability

$J_m(kr)$ \equiv m-order Bessel function

kr \equiv n-th root of the Bessel function of order m

L \equiv The length of the cavity

r \equiv distance from centre to any point before the wall of the cavity

E \equiv Electric field

B \equiv Magnetic field

ω_{nmp} \equiv Characteristic resonant frequencies

TE \equiv Transverse electric field

$\equiv R$ distance from centre to the wall of the

$f(r)$ Radial function

$\equiv p$ Axial mode

1.0 INTRODUCTION

In recent times, scientific applications of cylindrical cavities are rapidly evolving.

Cylindrical cavities are simply short circuited waveguides at both ends (Tarmizi-Ali et al., 2006), representing a very important group of microwave components.

Their applications range from the use as frequency metres and filters to tools for characterizing properties of materials (Itoh, 1974; Kean and Green, 1995; Raveendranath et al., 2000; Shao and Wang, 2007; Kandasamy and Okamoto, 2001).

Infinite numbers of resonant frequencies exist within a resonant cavity so that each

frequency is represented in its own mode. The lowest resonant frequency is known as the fundamental mode while the rest are known as the higher modes (Jackson, 1974). Every single mode of the cavity has in general its own distribution or form of field within the cavity.

This paper analyzes the performance of a cylindrical cavity at microwave frequencies, employing numerical approach. The thrust of the paper is to provide a useful guide for the engineering designs of high performance resonant cavity. The study provides insights into Bessel differential equation and the theory of cylindrical resonant cavity. The distribution of electric fields inside the cavity was numerically computed. Thereafter, numerical simulation for several excitation modes was carried out.

Section 2.0 provides useful insights into the theory of cylindrical resonant cavity. The numerical results and the discussions are presented in sections 3.0 and 4.0 respectively. The conclusion is finally drawn in section 5.0, and then the Appendix.

2.0 THE CYLINDRICAL CAVITY

Figure 1 shows the geometry of a typical cylindrical resonant cavity. The cavity is assumed to be homogeneously corrugated with material of dielectric permittivity ϵ , and permeability μ .

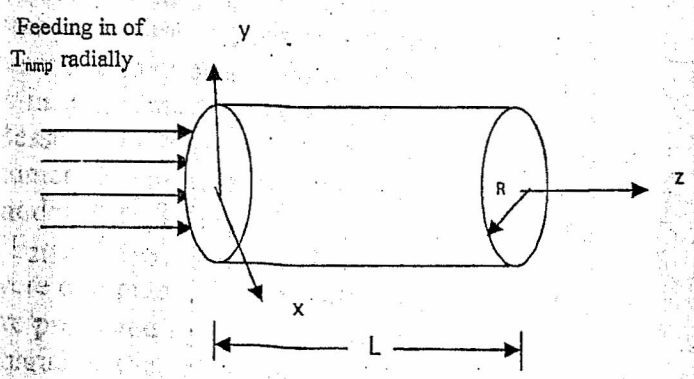


Figure 1: Geometry of a Typical Cylindrical Resonant Cavity

Considering time dependent sinusoids $e^{-i\omega t}$ for the fields inside the cavity (Jackson, 1974), the Maxwell equations can be expressed as:

$$\left. \begin{aligned} \nabla \times \mathbf{E} &= \frac{i\omega}{c} \mathbf{B} & \nabla \cdot \mathbf{B} &= 0 \\ \nabla \times \mathbf{B} &= -i\mu\epsilon \frac{\omega}{c} \mathbf{E} & \nabla \cdot \mathbf{E} &= 0 \end{aligned} \right\} \dots\dots\dots(3)$$

The fields obey the general wave equation so that; $\nabla^2 \mathbf{E} = 1/c^2 \partial^2 \mathbf{E} / \partial t^2$. In cylindrical coordinate system, and suppressing the angular dependence, the wave equation can be expressed as,

$$\frac{1}{r} \frac{\partial}{\partial r} \left(r \frac{\partial \mathbf{E}}{\partial r} \right) + \frac{\partial^2 \mathbf{E}}{\partial z^2} = \frac{1}{c^2} \frac{\partial^2 \mathbf{E}}{\partial t^2} \dots\dots\dots(4)$$

The general solutions of Equation (4) are of the form;

$$\mathbf{E} = \mathbf{E}_0(f(r)) \left\{ \begin{aligned} &\sin\left(\frac{p\pi z}{L}\right) \\ &\cos\left(\frac{p\pi z}{L}\right) \end{aligned} \right\} e^{-i\omega t} \dots\dots\dots(5)$$

The wave is fed radially into the cavity, but in z-direction. To this end, Equation (5) is subject to boundary conditions, $z=0$ and $z=L$ at the initial time $t=0$ to time $t=t$ when the waves emerge from the other end of the cavity. Consequently, the solution with $\cos(p\pi z/L)$ satisfies Equation (4) under the above boundary and initial conditions. Hence, the solution with $\sin(p\pi z/L)$ is suppressed so that,

$$\mathbf{E} = \mathbf{E}_0(f(r)) \cos\left(\frac{p\pi z}{L}\right) e^{-i\omega t} \dots\dots\dots(6a)$$

becomes the satisfactory solution. Therefore,

$$\frac{d^2 \mathbf{E}}{d(kr)^2} + \frac{1}{kr} \frac{d\mathbf{E}}{d(kr)} + \mathbf{E} = 0 \dots\dots\dots(7)$$

Where, $k^2 = \omega^2/c^2 - p^2\pi^2/L^2$

and p is the axial mode number of the cavity, c is the speed of light. Equation (7) is a Bessel differential equation with solutions $J_m(kr)$. The satisfactory solution of Equation (4) in terms of the m -order Bessel function is,

$$\mathbf{E} = \mathbf{E}_0 J_m(kr) \cos\left(\frac{p\pi z}{L}\right) e^{-i\omega t} \dots\dots\dots(6b)$$

In Equation (6b), kr is the n -th root of the Bessel function of order m . Hence, $\xi_n = kr$, but the function finally vanishes at $\xi_n = kR$. Then, from Equation (7), the characteristic resonant frequencies can be expressed as:

$$\omega_{nmp} = \frac{c}{L} \left\{ \left(\frac{L}{R} \right)^2 \xi_n^2 + p^2 \pi^2 \right\}^{\frac{1}{2}}$$

$$\left. \begin{matrix} p = m = 0, 1, 2, 3, \dots \\ n = 1, 2, 3, \dots \end{matrix} \right\} \dots \dots \dots (8)$$

The derivation of Equation (8) is shown in Appendix A.

3.0 NUMERICAL RESULTS

The cylindrical cavity is assumed to have dimensions $R=300\text{mm}$ and $L=450\text{mm}$. These dimensions are readily adjustable (tuneable) to achieve desirable characteristic resonant frequencies. The excitation modes, represented by TE_{nmp} mode; where n and m are positive integers, defining the root and the order of Bessel function respectively, and p is the axial mode of the excitation are radially fed through one of the opened ends of the cylinder so that the output comes out through the other end. The Bessel function shown in Equation (6b) was numerically computed to finally determine the state of the electric field distribution for the radial excitation. The result of this computation is shown below (Figure 2).

The characteristic resonant frequency expression shown in Equation (8) was used to compute the corresponding fundamental resonant frequency. Since the initial excitation is in TE_{111} mode, the first root of the 1st order Bessel function was considered. Thereafter, numerical simulation of other higher excitation modes (i.e. TE_{112} , TE_{113} , TE_{114} , TE_{115} , TE_{116} ; TE_{211} , TE_{212} , TE_{213} , TE_{214} , TE_{215} and TE_{216} were computed. The results of the computations are presented by Figure 3 (a-d)). The associated characteristic resonant frequencies when the dimensions of the cavity are arbitrarily varied (in length-radius ratio) are also extrapolated.

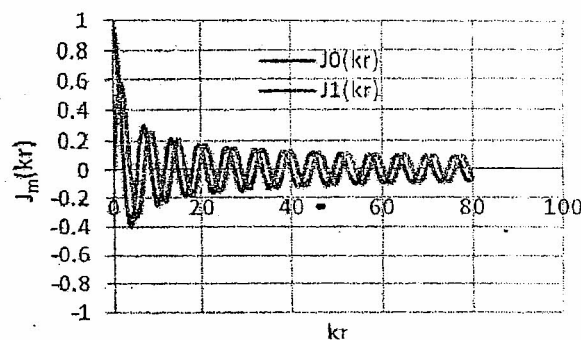


Figure 2: Bessel functions showing the radial excitation of the fields within the resonator.

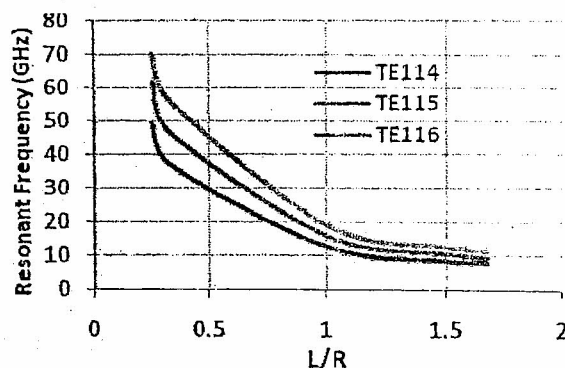


Figure 3a: Plots of the Resonant Frequency versus the Ratio of the Length of the Cavity to its Radius at TE_{114} , TE_{115} , and TE_{116} Modes.

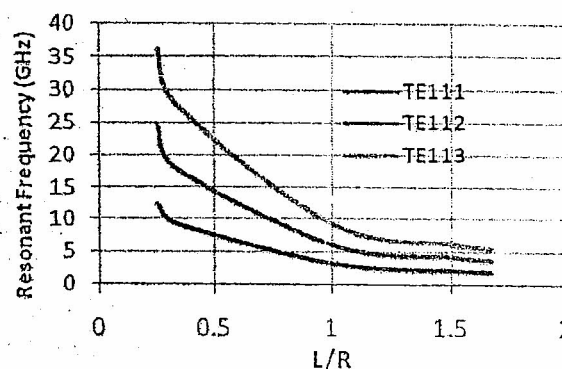


Figure 3b: Plots of the Resonant Frequency versus the Ratio of the Length of the Cavity to its Radius at TE_{111} , TE_{112} , and TE_{113} Modes.

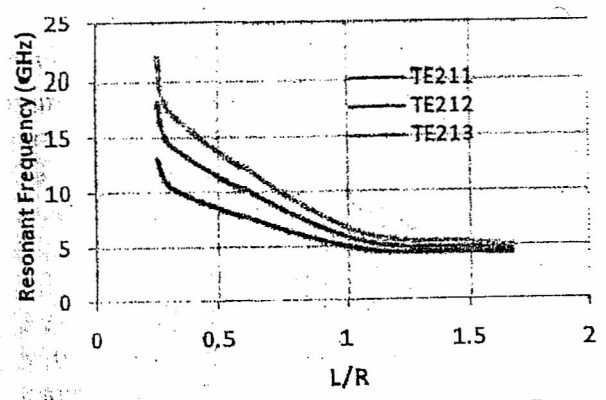


Figure 3c: Plots of the Resonant Frequency versus the Ratio of the Length of the Cavity to its Radius at TE_{211} , TE_{212} , and TE_{213} Modes.

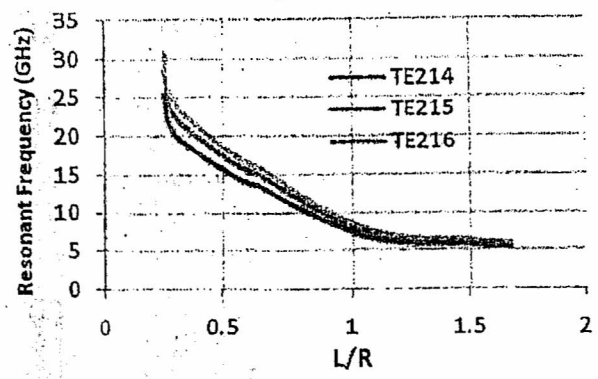


Figure 3d: Plots of the Resonant Frequency versus the Ratio of the Length of the Cavity to its Radius at TE_{214} , TE_{215} , and TE_{216} Modes.

0 DISCUSSION

The radial distribution of the fields within the resonant cavity can be explained by the Bessel function shown in Figure 2. Within the centre of the cavity ($r \rightarrow 0$), the field strength attains maximum magnitude and diminishes as $r \rightarrow R$ (around the wall of the cavity). In other words, the distribution of the fields within the cavity for any specific fundamental frequency is uneven; i. e. strong within the centre and diminishes towards the walls of the cavity. Homogenous distribution of the fields can be attained by inserting relevant dielectric materials at the centre of the cavity with the view to establishing hybrid modes (Orfanidis et al., 2007).

Following a different approach from the technique suggested by Orfanidis et al. (2007),

the present study considers simulation of several excitation modes for the overall interest of selecting preferred mode (mode matching) for any particular predetermined resonant frequency of choice.

The characteristic resonant frequencies at various modes (TE_{nlp}) were computed using the n-th roots of the Bessel function of order m that are shown in Figure 2. The first step considers $n=1$ and $p=1, 2, 3, \dots, 6$ at $m=1$; and the second step considers $n=2$ and $p=1, 2, 3, \dots, 6$ at $m=1$. The results of the calculated resonant frequency for each mode at varying length-radius (L/R) ratio were plotted in Figures 3(a-d). All the plots are quasi-linear and similar in behaviour: they are continuous with sharp descent in the resonant frequency with respect to L/R ratio at points less than 0.5. This descent becomes relatively steady between 0.5 and 1.5, and near-uniform variation at points greater than 1.5. This point, where the cavity shows near-uniform resonant frequency for TE_{nlp} mode is in reasonable agreement with L/R ratio of less than 2.03 that was suggested by Tarmizi-Ali et al. (2006).

Another important observation from the plots is the marked increase in the resonant frequency with increase in the excitation modes at L/R ratio less than 0.5, and grows towards steadiness in variation as L/R move above 1.5. Overall, it is important to highlight the preference of L/R greater than 1.5, and better choice of modes for a predetermined resonant frequency as the significant indices for designing a robust system. Besides, in order to mitigate the effects of uneven distribution of fields within the cavity, the possibility of incorporating multiple feeders (i. e. multiple waveguides) as the excitation source for the overall improvement of the field distribution within the cavity may be an excellent option.

5.0 CONCLUSION

The performance of cylindrical cavities at microwave frequencies was analyzed using numerical approach, with the view to providing useful guides for the engineering designs of high performance resonant cavity.

The distribution of electric fields inside the cavity was numerically computed. Thereafter, numerical simulation for several excitation modes was carried out. Analysis of the results from the numerical computations leads to the conclusion that, $L/R > 1.5$, and proper choice of modes (mode matching) are the significant indices for designing a robust system. The present study intuitively suggests the possibility of incorporating multiple feeders (i. e. multiple waveguides) as the excitation source for the overall improvement of the field distribution within the cavity so as to reduce the effects of uneven distribution of fields within the cavity.

REFERENCES

- (1) Itoh, T. (1974): A New Method for Measuring Properties of Dielectric Material Using a Micro-strip Cavity, *IEEE Trans. on Microwave Theory and Techniques*, (short papers).
- (2) Jackson J. D. (1974): Classical Electrodynamics, 2nd edn., John Wiley & Sons, NY, U.S.A.
- (3) Kandasamy, P. and N. Okamoto, (2001): Resonant modes of a concentric spherical cavity with conically stratified medium, *IEEE Trans. on Microwave Theory and Techniques*, **49**(1), pp. 111 – 118.
- (4) Keam, R. and A. D. Green (1995): Measurement of Complex Dielectric Permittivity at Microwave Frequencies Using a Cylindrical Cavity, *Electronics Letters*, **31**(3), pp. 212-214.
- (5) Kreyszig, E. (2005): Advanced Engineering Mathematics, 8th edn., John Wiley & Sons (Asia) Pte Ltd., Singapore.
- (6) Orfanidis, A. P., G. A. Kyriacou, and J. N. Sahalos (2007): Numerical Analysis of Cylindrical Cavities Used for Microwave Heating, Employing the Mode Matching Technique, *Piers Online*, **3**(8), pp. 1228-1231.
- (7) Raveendranath, U., S. Bijukumar, and K. T. Mathew (2000): Broadband Coaxial Cavity Resonators for Complex Permittivity Measurements of Liquids, Instrumentation and Measurement, *IEEE Transactions* **49**(6), pp. 1305-1312.
- (8) Shao, W. And B. Z. Wang (2007): Order-Marching Time Domain Method in Cylindrical Coordinate System for Eigen-value Problems, *J. Electromagnetic waves and Applications*, **21**(14), pp. 2025-2031.
- (9) Tarmizi-Ali, M., M. Mohd-Salleh, and M. M. Md-Zan (2006): Air-Filled Circular Cross Sectional Cavity for Microwave Non-Destructive Testing, *World Academy of Science, Engineering and Technology*, **18**, pp. 107-112.

APPENDIX A

The satisfactory solution of Equation (4) is given in Equation (6b). From Equation (6b), the Bessel function of order m has roots for different values of kr . However, at $r=R$ (within the walls of the cavity), the Bessel function vanishes so that,

$$J_m(kR) = 0 \quad (A1)$$

Defining the n -th root of the Bessel function as $\xi_n = kr$, so that the function finally vanishes at $\xi_n = kR$. This implies that,

$$k = \frac{\xi_n}{R} \quad (A2)$$

From Equation (7), k^2 has been defined as $k^2 = \omega^2/c^2 - p^2\pi^2/L^2$. Therefore, k in Equation (A2) can be substituted to obtain,

$$\frac{\omega^2}{c^2} = \frac{\xi_n^2}{R^2} + \frac{p^2\pi^2}{L^2} \quad (A3)$$

From Equation (A3), the characteristic equation for the resonant frequency is,

$$\omega_{nmp} = \frac{c}{L} \left\{ \left(\frac{L}{R} \right)^2 \xi_n^2 + p^2\pi^2 \right\}^{\frac{1}{2}}$$